

Specific protein methylation defects and gene expression perturbations in coactivator-associated arginine methyltransferase 1-deficient mice

Neelu Yadav^{*†}, Jaeho Lee^{*†}, Jeesun Kim^{*}, Jianjun Shen^{*}, Mickey C.-T. Hu[‡], C. Marcelo Aldaz^{*}, and Mark T. Bedford^{*§}

^{*}Department of Carcinogenesis, University of Texas M. D. Anderson Cancer Center, P.O. Box 389, Smithville, TX 78957; and [‡]Department of Molecular and Cellular Oncology, University of Texas M. D. Anderson Cancer Center, 1515 Holcombe Boulevard, Houston, TX 77030

Communicated by Philip Leder, Harvard Medical School, Boston, MA, April 17, 2003 (received for review February 25, 2003)

Arginine methylation has been implicated in the regulation of gene expression. The coactivator-associated arginine methyltransferase 1 (CARM1/PRMT4) binds the p160 family of steroid receptor coactivators (SRCs). This association enhances transcriptional activation by nuclear receptors. Here, we show that embryos with a targeted disruption of CARM1 are small in size and die perinatally. The methylation of two known CARM1 substrates, poly(A)-binding protein (PABP1) and the transcriptional cofactor p300, was abolished in knockout embryos and cells. However, CARM1-dependent methylation of histone H3 was not observed. Furthermore, estrogen-responsive gene expression was aberrant in *Carm1*^{-/-} fibroblasts and embryos, thus emphasizing the role of arginine methylation as a transcription activation tag. These findings provide genetic evidence for the essential role of CARM1 in estrogen-mediated transcriptional activation.

arginine methylation | CARM1 | p300 | PABP | estrogen

In eukaryotic cells, proteins can be methylated on the side-chain nitrogens of the amino acids arginine, lysine, and histidine (1). The methylation of arginine residues is catalyzed by at least two different classes of protein arginine methyltransferase (PRMT) enzymes. The type I enzymes catalyze the formation of asymmetric *N*^G,*N*^G-dimethylarginine residues, and the type II enzyme catalyzes the formation of symmetric *N*^G,*N*^G-dimethylarginine residues (2). PRMTs have been implicated in a variety of processes, including cell proliferation, signal transduction, and protein trafficking (3). In mammals, five type I enzymes (PRMT1, -2, -3, -4, and -6; refs. 4–8) and a single type II enzyme (PRMT5; refs. 9 and 10) have been described.

The identification of coactivator-associated arginine methyltransferase 1 (CARM1; PRMT4) as a GRIP1 (glucocorticoid receptor-interacting protein 1)-binding protein led to studies showing that this methyltransferase can stimulate transcriptional activation by nuclear receptors in combination with the p160 family of coactivators (7). Subsequent work has demonstrated that PRMT1 also has coactivator activity that functions synergistically with CARM1 (11, 12). The abilities of PRMT1 to methylate histone H4 and of CARM1 to methylate histone H3 suggest that these enzymes contribute to the histone “code” (13–15). Indeed, the methylation of histone H4 by PRMT1 facilitates subsequent acetylation by p300 (16), possibly influencing chromatin remodeling. The opposite observation has been made for H3 methylation, where prior acetylation of H3 by CREB-binding protein (CBP) facilitates its methylation by CARM1 (17). CARM1’s coactivator activity is not dedicated to transactivated steroid receptors but also functions with the myogenic transcription factor mouse embryonic fibroblast (MEF) 2C (18) and β -catenin (19). Chromatin immunoprecipitation analysis has shown that histone H3 becomes methylated *in vivo* on Arg-17 at the estrogen receptor-regulated pS2 gene (20) and at a genome integrated mouse mammary tumor virus (MMTV) reporter (21), and this meth-

ylation coincides with the presence of CARM1. CARM1 methylates not only histone H3 but also poly(A)-binding protein 1 (PABP1; ref. 22) and the transcriptional cofactors CBP/p300 (23, 24). Thus, CARM1 may regulate multiple aspects of gene-specific activation, including histone methylation and acetylation, as well as general transcript integrity.

Materials and Methods

Targeting Vector Construction. Genomic DNA was isolated from a 129 BAC (bacterial artificial chromosome) library (Research Genetics, Huntsville, AL) by using the full-length mouse CARM1 cDNA as a probe. A 7-kb *Eco*RI fragment containing two CARM1 exons (encoding amino acids 117–187) was subcloned into Bluescript and sequenced. First, a loxP sequence and a new *Bam*HI site were introduced into the genomic sequence at a unique *Bgl*III site. A 3.9-kb genomic fragment, containing two exons and the introduced loxP site, was generated by PCR and cloned into the *Sac*II site of the “flrtd” neomycin-resistance (Neo) expression cassette pM-11 (25), to generate the right arm. The pM-11 cassette contains a single loxP site in the same orientation as the loxP site that was engineered into the genomic sequence of the right arm. The left arm (2.1 kb) was also generated by PCR, and the resulting product was inserted into *Sal*I and *Kpn*I sites between the diphtheria toxin A-chain gene (DT) (26) and the neo expression cassette (25). This cloning event generated the final pKO-CARM1 targeting vector containing 6 kb of CARM1 genomic DNA. Roughly 600 bp from the 3’ genomic sequence was subcloned for use as an external probe. The PCR primers used to generate the external probe are 5’-CTA AAG TCC TAG CAG CAG TGC-3’ and 5’-CCA GCT TAA CAC AGT GAG ACC-3’.

Gene Targeting, Embryonic Stem (ES) Cell Culture, and Generation of CARM1 Mice. TC-1 ES cells were electroporated with *Pvu*I-linearized pKO-CARM1 and selected in G418 (27). Genomic DNA from 200 neomycin-resistant colonies was screened for homologous recombination by *Bam*HI digestion and Southern blot hybridization with an external probe. Five clones were found to be correctly targeted. Chimeric mice were generated by the morula-ES cell aggregation technique (28). High-grade chimeric mice have been made successfully with the ES cell line 1.13. Males with a high contribution of ES cells were crossed with Black Swiss females to generate agouti F1s, thus demonstrating that the manipulated ES cells had undergone germ-line transmission. For timed pregnancies, *Carm1*^{+/-}

Abbreviations: CARM1, coactivator-associated arginine methyltransferase 1; PRMT, protein arginine methyltransferase; PABP1, poly(A)-binding protein 1; MEF, mouse embryonic fibroblast; GAR, glycine- and arginine-rich; ES, embryonic stem; En, day *n* of gestation.

[†]N.Y. and J.L. contributed equally to this work.

[§]To whom correspondence should be addressed at: University of Texas M. D. Anderson Cancer Center, Park Road 1-C, P.O. Box 389, Smithville, TX 78957. E-mail: mbedford@sprd1.mdacc.tmc.edu.

mice were mated overnight. Females were inspected for vaginal plugs the following morning, and noon was taken as day 0.5 of gestation (E0.5).

CARM1 MEF Cultures and Stable Transfections. Individual embryos from *Carm1*^{+/-} intercrosses at E12.5 were placed into culture as described (29). Cells were maintained on a 3T3-culture protocol in which 10⁶ cells were passed onto a gelatinized 10-cm dish every 3 days. Stable lines (20-1 and 20-3) were established by transfection of the *Carm1*^{-/-} lines 20 with pCAGGS-FLPe-puro, which was developed by F. Stewart (European Molecular Biology Laboratory) and a gift from S. Dymecki (Harvard Medical School, Boston).

Luciferase Assays and Transient MEF Transfections. ERE-TK-Luc has a single vitellogenin estrogen response element containing a basal herpes simplex virus thymidine kinase (TK) promoter linked to firefly luciferase (30). pT7E2 contains human estrogen receptor driven by RSV promoter (30). pCMV-renilla has renilla luciferase driven by a CMV promoter (Promega). MEFs were maintained in DMEM supplemented with 10% FBS. Approximately 20 h before transfection, 40,000 cells were seeded into each well of 12-well culture dishes. The cells in each well were transfected with FuGENE 6 transfection reagent (Roche Applied Science, Indianapolis, IN) according to the manufacturer's protocol. For each transfection, 25 ng of pCMV-renilla, 335 ng of estrogen receptor, and 40 ng of ERE-TK-Luc were used. Total DNA in each well was adjusted to 400 ng with plasmid Bluescript where needed. After 4 h of transfection, the cells were washed twice with PBS and grown in phenol red free DMEM supplemented with 5% charcoal striped FBS and treated with 10 nM estradiol (Sigma). After 42–44 h, the cells were washed twice with PBS and harvested to perform luciferase assay by using the Dual Luciferase Assay System (Promega).

Histological Analysis. Embryos with their abdomens perforated were fixed in formalin and embedded in paraffin wax. Embryos were sectioned at 3 μm and subjected to immunohistochemical localization of CARM1 (1:20) and dimethylated [Arg-17]-histone H3 (1:100). Staining was performed by using the En-Vision system (DAKO), and the counterstain was hematoxylin.

Antibodies. The antibody against PABP1 was a gift from N. Sonenberg (McGill University, Toronto). The antibodies against CARM1 and dimethylated-histone H3 (Arg-17) are available commercially (Upstate Biotechnology, Lake Placid, NY) as are antibodies against mouse complement C3 (ICN). Antibodies against STC2 were raised in rabbits to the peptide sequence: CMHFKDLLLHEPYVIDG (Bethyl Laboratories, Montgomery, TX).

GST Fusion Proteins. GST-glycine- and arginine-rich (GAR) has been described (2) and contains the GAR domain of fibrillarin. GST-PABP has been described (22). GST-p300 contains the KIX domain of p300, and the expression construct was generated by PCR from a pCMVβ-p300 template by using the following oligonucleotide set: 5'-TAA GTC GAC TTA ACA TGG GTC AAC AGC CAG CC-3' and 5'-TGA GCG GCC GCT CAG GAA GAA CTA GAC ATT TGT GC-3'. The resulting PCR product was cloned into *SalI* and *NotI* sites of pGEX-6P-1 (Amersham Biosciences). GST fusion proteins were prepared as described (8).

In Vitro Methylation Assay. MEF lines were grown to 80% confluency on a 10-cm plate. Cells were washed with PBS and scraped off the plate into 500 μl of PBS (pH 7.4). Cells were lysed by sonication, and the supernatant was used as the

enzyme source. *In vitro* methylation reactions were performed by adding the cell lysate to 1 μg of GST fusion protein bound to glutathione beads in the presence of 2 μl of the methyl donor *S*-adenosyl-L-[methyl-³H]methionine ([³H]AdoMet) [79 Ci/mmol (1 Ci = 37 GBq) from a 12.6-μM stock solution; Amersham Biosciences]. The reaction was incubated at 30°C for 1 h, and then the beads were washed three times with PBS. The substrate-bound beads were suspended in protein running buffer and boiled, and the samples were separated on a 10% SDS/PAGE, transferred to a poly(vinylidene difluoride) membrane, sprayed with Enhance (NEN), and exposed to film overnight.

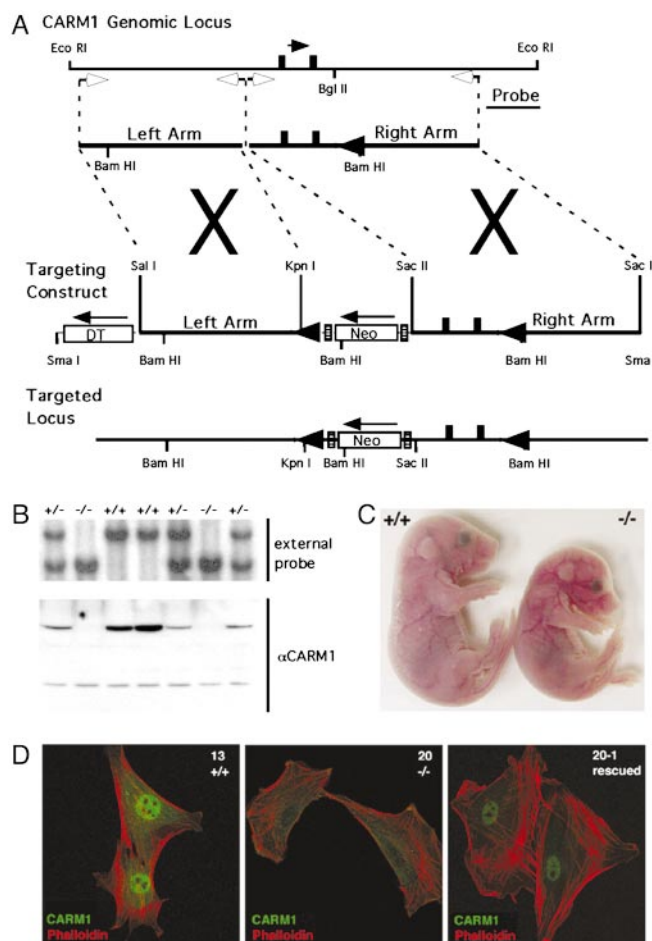


Fig. 1. Targeted disruption of *Carm1* gene. (A) Strategy for homologous recombination of the *Carm1* genomic locus. Position of the external probe is shown. A *neo* cassette flanked by *flp* sites was introduced into the intronic region. Two *Carm1* exons, which encode a portion of the substrate-binding region, were floxed. Arrowheads depict *loxP* sites, solid boxes depict exons, and hatched boxes depict *flp* sites. Filled arrows depict direction of transcription, and open arrows depict the position of PCR primers used to generate the arms of the targeting construct. (B) A litter of E12.5 embryos was analyzed for gene targeting. Genomic DNA was isolated from embryo trunk, digested with *Bam*HI, and analyzed by Southern blotting by using the 3' external probe (Upper). Protein was extracted from the heads of the same embryo set and subjected to Western blot analysis by using an αCARM1 antibody, demonstrating the absence of CARM1 immunoreactive staining in mutant embryos (Lower). (C) Embryonic (E18.5) size difference of wild-type (+/+) and *Carm1* mutant (-/-) mice. (D) Subcellular localization of CARM1 protein in mutant (-/-) and wild-type (+/+) cells. Confocal microscope image of wild-type (13^{+/+}), *Carm1* mutant (20^{-/-}), and Flpase rescued (20-1 rescued) MEF cell lines processed for immunostaining with αCARM1 primary antibody, an FITC-conjugated secondary antibody and Texas red-conjugated phalloidin.

Table 1. Genotypes of offspring from *Carm1*^{+/-} intercrosses

Age	Total offspring	Genotype		
		+/+	+/-	-/-
E8.5–12.5	152	37	82	33 (21.7)
E13.5–15.5	41	11	17	13 (31.7)
E18.5–19.5	249	80	135	34 (13.5)
P1	149	45	92	12* (8.0)
Weaning	292	139	153	0 (0.0)

Embryos and neonates were harvested at the times indicated. Genomic DNA was extracted and subjected to Southern blot analysis to determine the genotype. Parentheses indicate percentage of -/- genotype. *Indicates dead pups.

Acid Extraction of Histones. MEF lines were grown to 80% confluency. Cells were suspended in RSB (10 mM Tris-HCl, pH 7.4/10 mM NaCl/3 mM MgCl₂) and then centrifuged. The pellet was resuspended in RSB plus 0.5% Nonidet P-40, placed on ice for 10 min, and then centrifuged again (500 × g). Nuclei were resuspended in 5 mM MgCl₂, and an equal volume of 0.8 M HCl was added, and histones were extracted for 20 min on ice. Histones (in supernatant) were precipitated with 25% (wt/vol) trichloroacetic acid and centrifuged at 8,000 × g. The pellet was washed twice with cold acetone and then resuspended in deionized water.

In Vivo Methylation Assay. MEFs were labeled by using a previously described *in vivo* methylation assay (31). The cells were lysed in RIPA buffer (0.15 mM NaCl/0.05 mM Tris-HCl, pH 8/0.5% sodium deoxycholate/1% NP-40/0.1% SDS), and immunoprecipitations were performed with αPABP antibodies. Samples were separated on a 10% SDS/PAGE, transferred to a poly(vinylidene difluoride) membrane, sprayed with Enhance (NEN), and exposed to film overnight.

Results

Neonatal Lethality in Mice Deficient in CARM1. To characterize the biological function of CARM1, we generated *Carm1*^{-/-} mice by gene targeting. The targeting vector was generated by introducing a neomycin-resistance (*neo*) cassette (25), flanked by *frt* sites,

into an intronic region. Two exons that encode for 71 aa were flanked with *loxP* sites to allow us to perform tissue-specific knockout experiments in the future (Fig. 1A). The deletion of this coding region (amino acids 117–187) will remove a three-helix segment that is involved in cofactor binding (AdoMet), and forms part of the Rossmann fold (32, 33). Correctly targeted clones were identified by Southern blot hybridization. Targeted ES cells were used to generate chimeric mice that were then bred to generate heterozygous progeny.

Carm1^{+/-} mice were normal and fertile, and were intercrossed to produce *Carm1*^{-/-} mice. No nullizygous mice were detected at weaning, indicating that loss of CARM1 causes recessive lethality (Table 1). Neonates and embryos from heterozygote intercrosses were analyzed by Southern blot, and mice of the expected genotypes were obtained at a normal Mendelian ratio before stage E15.5. At 12.5 days (E12.5) of gestation, *Carm1*^{-/-} embryos (Fig. 1B Upper) are grossly normal (data not shown), even though they express no detectable CARM1 protein (Fig. 1B Lower). The fact that no protein expression is seen in *Carm1*^{-/-} homozygous embryos indicates that the introduction of the *neo* cassette into the *Carm1* intronic sequence was sufficient to disrupt this allele. At E18.5 and E19.5, the number of *Carm1*^{-/-} embryos was lower than expected (13.5%), indicating some embryonic lethality (Table 1). Stage E18.5 *Carm1*^{-/-} embryos are significantly smaller (~60%) than their wild-type littermates but are still grossly normal (Fig. 1C). On the day of birth, we have identified dead *Carm1*^{-/-} pups. To determine whether *Carm1*^{-/-} embryos die before birth, we dissected E19.5 embryos from uteri of *Carm1*^{+/-} intercrosses. Unlike wild-type littermates, *Carm1*^{-/-} embryos isolated by Caesarian section failed to breathe, did not turn pink, but did respond to stimulus when pinched with forceps. Histological examination revealed that the lungs of the *Carm1*^{-/-} neonates failed to inflate with air and their alveolar air spaces were small as compared with wild-type littermates (data not shown). No other apparent histological abnormalities were observed. Thus *Carm1*^{-/-} embryos generally survive the entire course of development but die at the perinatal stage, emphasizing the essential nature of this enzyme. It should be noted that there seems to be a loss of *Carm1*^{+/-} pups between birth and weaning (Table 1). We expect twice the number of *Carm1*^{+/-} pups to wild-type pups

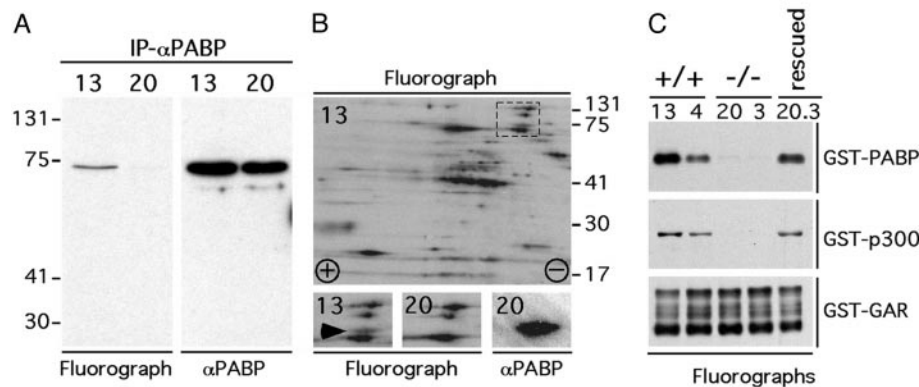


Fig. 2. Loss of PABP1 and p300 methylation in the absence of CARM1. (A) Methylated proteins in wild-type (13^{+/+}) and *Carm1* mutant (20^{-/-}) MEF cell lines were labeled *in vivo* (31). Immunoprecipitations (IP) were performed with an αPABP antibody. The ³H-labeled proteins were visualized by fluorography (Left), and the same membrane was immunoblotted with αPABP antibodies (Right). Protein A/G-horseradish peroxidase (HRP) was used as the secondary reagent. (B) Comparison of global protein methylation from wild-type (13^{+/+}) and *Carm1* mutant (20^{-/-}) MEF cell lines. Total protein (200 μg) from *in vivo*-labeled MEFs was subjected to 2D-gel analysis, over a 6–11 pH gradient, followed by fluorography. The framed region focuses on the location of PABP1. The location of PABP1 (arrowhead) in the 20^{-/-} line was determined by probing the fluorographed membrane with αPABP antibodies. (C) The CARM1 substrates p300 and PABP1 cannot be methylated when using CARM1 knockout cell extracts as an enzyme source. Wild-type (lines 13 and 4) and rescued (20.3) MEF extracts, but not extracts from knockout lines (lines 20 and 3), were able to methylate recombinant CARM1 substrates, GST-p300, and GST-PABP1. Both CARM1 knockout and wild-type cell line extracts methylated the PRMT1 substrate, GST-GAR.

but instead see close to a 1:1 ratio, suggesting some lethality even when a single copy of CARM1 is not functional.

To facilitate additional studies of CARM1 cellular functions, we cultured MEFs from E12.5 embryos. Two MEF lines of each genotype were established: *Carm1*^{+/+} lines 13 and 4, *Carm1*^{-/-} lines 10 and 8, and *Carm1*^{-/-} lines 20 and 3. In addition, two rescued lines (20.1 and 20.3) were also established by stable transfection of *Carm1*^{-/-} line 20 with a Flp/puro construct. The expression of Flp recombinase removed the *frt* flanked intronic *neo* cassette, which resulted in the reactivation of the CARM1 locus. The integrity of CARM1 expression in the established MEF lines was confirmed by Western (data not shown) and immunofluorescence analysis (Fig. 1D).

The Effect of CARM1 Loss on PABP1 and p300 Methylation. Proposed substrates for CARM1 include histone H3, the transcriptional cofactors CREB-binding protein/p300, and PABP1. To determine whether PABP1 was methylated in the absence of CARM1, we performed *in vivo* methylation reactions on *Carm1*^{+/+} MEFs and *Carm1*^{-/-} MEFs by incubating the cells with [methyl-³H]-L-methionine in the presence of the protein synthesis inhibitor cycloheximide (22, 31). PABP1 was immunoprecipitated from these labeled cell extracts. Equivalent amounts of PABP1 were present in both cell lines, but PABP1 from the wild-type line and not the knockout line was methylated (Fig. 2A). To visualize the loss of PABP1 methylation relative to other methylated proteins, we subjected [methyl-³H]-labeled MEFs to 2D PAGE (Fig. 2B). The large majority of methylated proteins remain unchanged, but PABP1 was not methylated in *Carm1*^{-/-} MEFs. Next, we used MEF extracts as a source of methyltransferase activity to transfer a tritium-labeled methyl group from AdoMet onto GST fusion proteins harboring the methylatable motifs of PABP1, p300, and the GAR motif of fibrillarin. Cell extracts from *Carm1*^{-/-} MEF lines were unable to methylate GST-PABP or GST-p300, but GST-GAR (an *in vitro* substrate for PRMT1, -3, and -6) was methylated by the knockout lines (Fig. 2C). These data indicate that no alternative pathways exist to rescue the loss of CARM1 activity.

Antiserum Specific for Methylated (Arg-17) Histone H3 Is a Marker for CARM1 Activity. CARM1 methylates histone H3 at Arg-17 *in vitro* (13), and, based on analysis with methyl-specific antibodies raised to this epitope, it has been demonstrated that the recruitment of CARM1 to an active promoter results in Arg-17 methylation *in vivo* (20, 21). The α -methyl[R17]H3 antibody recognizes calf thymus histone H3 methylated *in vitro* by CARM1 (Fig. 3A; ref. 21). The analysis of embryonic protein extracts further demonstrated that the α -methyl[R17]H3 antibody is immune-reactive in a CARM1-dependent fashion (Fig. 3B). This Western analysis revealed two prominent cross-reactive bands (\approx 135 kDa and 145 kDa) that are present in wild-type but not *Carm1*^{-/-} embryo protein extracts. These proteins are not the size of histone H3 or other known CARM1 targets (PABP and p300), indicating that they represent as yet unidentified CARM1 substrates. Furthermore, core histones purified from wild-type, *Carm1*^{-/-}, and rescued MEFs bound the α -methyl[R17]H3 antibody to the same degree (Fig. 3C), thus demonstrating that this methyl-specific antibody recognizes methylation changes in some CARM1 substrates (Fig. 3B) but not histone H3 (Fig. 3C).

We then reasoned that, if CARM1 is responsible for generating methyl-dependent binding sites for the α -methyl[R17]H3 antibody, then CARM1 will colocalize with α -methyl[R17]H3 antibody immune-reactivity in tissues. This result is indeed what was observed by immunohistochemical studies. CARM1 was widely expressed in multiple tissues that also were sites of α -methyl[R17]H3 immune-reactivity (Fig. 3D). Importantly,

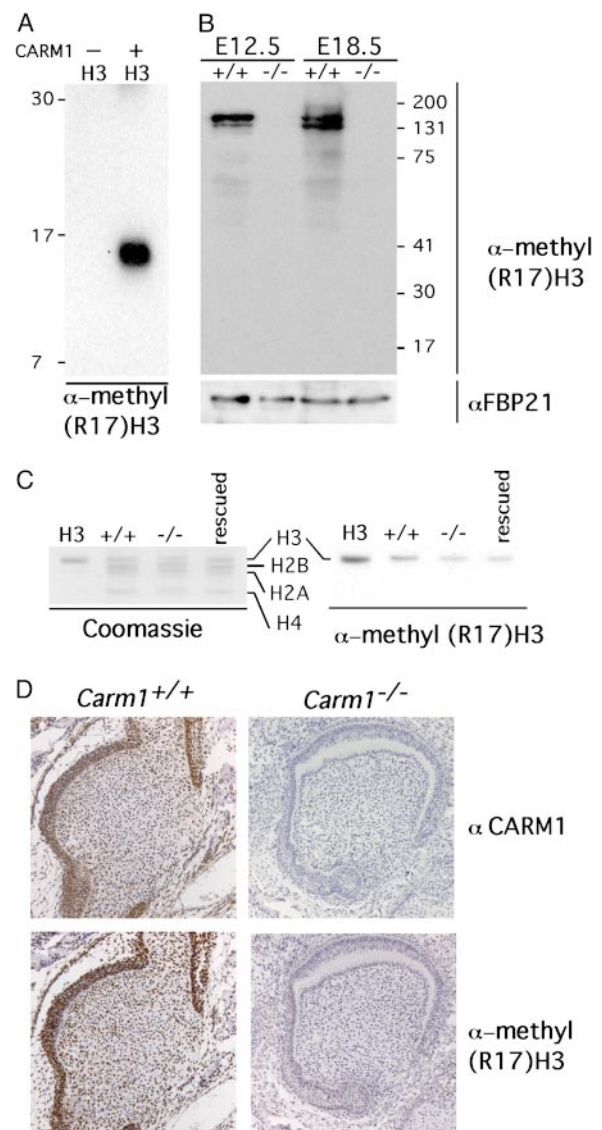


Fig. 3. Loss of CARM1 affects the immune-reactivity of an antibody specific for methylated histone H3 (α -methyl[R17]H3). (A) Immunoblot of purified calf thymus histone H3 before and after incubation with AdoMet and recombinant GST-CARM1 (10-s exposure). (B) Immunoblot of total protein lysates prepared from E12.5 and E18.5 embryos by using α -methyl[R17]H3 (Upper) and α -FBP21 (Lower, loading control; ref. 39). (C) Acid-purified core histones from MEF cell lines 13^{+/+}, 20^{-/-}, and 20.3 (rescued) Coomassie-stained as a loading control (Left) and an immunoblot by using α -methyl[R17]H3 (7-min exposure; Right). (D) Immunohistochemical localization of CARM1 and α -methyl[R17]H3 reactivity in *Carm1*^{+/+} and *Carm1*^{-/-} embryos at day E18.5 viewed at \times 100 magnification. This view represents the primordium of the upper incisor tooth.

CARM1 and α -methyl[R17]H3 staining were absent in *Carm1*^{-/-} embryos.

CARM1 Is Required for Estrogen-Dependent Transcription. It has been shown that CARM1 enhanced GRIP1's coactivator function for nuclear hormone receptors (7). We thus went on to examine whether CARM1 is required for estrogen-dependent transcription. We used a panel of MEF lines to determine the effect of CARM1 loss on hormone-dependent activation of reporter genes by the estrogen receptor ER- α (Fig. 4A). Reporter activity was largely absent in the *Carm1*^{-/-} MEF lines (lines 20 and 3) but was reestablished in rescued

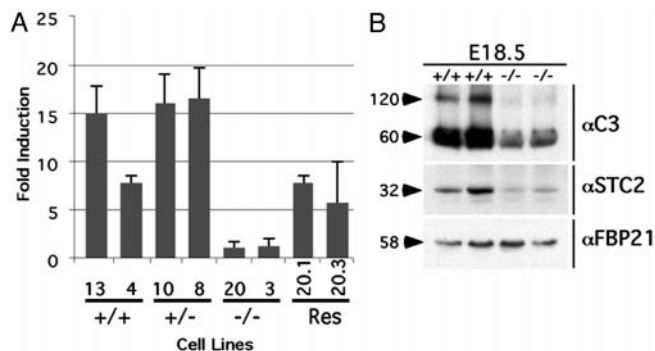


Fig. 4. CARM1 is involved in estrogen receptor-mediated transactivation of a luciferase reporter in MEF cells and endogenous targets in embryos. (A) A panel of MEFs was tested for their ability to transactivate a vitellogenin estrogen response element. Cell lines were transiently transfected with estrogen receptor (ER α), vitERE-TK-Luc reporter, and renilla (control). After transfection, cells were grown in charcoal striped serum and treated with 10 nM estradiol. Relative activity of firefly luciferase was normalized against renilla luciferase activity, and the results were expressed as fold induction of luciferase activity on treatment with hormone. The results are expressed as the mean \pm SD of three independent experiments done in triplicate. (B) Immunoblot of total protein lysates prepared from E18.5 embryos by using α -complement C3 (Top), α -STC2 (Middle), and α -FBP21 (Bottom, loading control). Sizes of immune-reactive bands are labeled in kDa.

MEF lines (20-1 and 20-3). Thus, CARM1 functions as a key component of estrogen receptor transactivation. It is probable that, because all of the steroid receptor coactivators (SRCs) bind and recruit CARM1 (7), the requirement of CARM1 for SRC-mediated coactivation is critical as it seems to act as a point of convergence. Furthermore, the reliance on CARM1 for ER-mediated gene expression is also observed *in vivo* at the protein level (Fig. 4B). Known estrogen-regulated genes, including complement C3 (34, 35) and STC2 (36, 37), were expressed at much-reduced levels in *Carm1*^{-/-} embryo extracts. Other targets for estrogen action, like the progesterone receptor, were not detected by immunoblotting, probably due to low abundance at this time in mouse development.

Discussion

In this study, we demonstrate that mice deficient in CARM1 die during late embryonic development or immediately after

birth. The ubiquitous expression of CARM1, the synergistic nature of CARM1 with a host of transcription pathways (18, 19, 38), and the runt phenotype of the mutant embryos suggest that this PRMT plays a broader role in the regulation of transcription. CARM1 is a highly specific enzyme that methylates a distinct class of substrates not recognized by PRMT1, -3, -5, or -6 (8). Methylation of the CARM1 substrates PABP1 and p300 is not supported by extracts from knockout cells. We have purified core histones and were unable to detect changes in histone H3 methylation status in *Carm1*^{-/-} embryos (data not shown) or in *Carm1*^{-/-} MEFs (Fig. 3C), using an α -methyl[R17]H3 antibody. The steady state *in vivo* levels of both histone H4 methylation at Arg-3 by PRMT1 (14, 16) and histone H3 methylation at Arg-17 by CARM1 (21) are low. It has been estimated that calf thymus H3 molecules harbor 3–4% methylated arginine residues (13). One would expect that a methyl-specific antibody would discriminate between Coomassie-stainable amounts of methylated and unmethylated H3, even at these low levels of methylation (3–4% vs. 0%). Thus, chromatin immunoprecipitation experiments with this antibody will at best detect DNA associated with unknown methylated CARM1 substrates (Fig. 3B) along with histone H3. To identify clear differences in the histone H3 “code,” we may have to focus on hormone responsive tissues, and these studies will be pursued by using the “conditional” nature of the CARM1 knockout model described here.

In summary, through its disparate substrate choice, CARM1 plays a complex role in controlling gene expression, with targets that regulate transcription (p300), DNA packaging (histone H3), and mRNA stability and translation (PABP1). Most importantly, the expression of complement C3 and STC2, two genes that are regulated by estrogen, was reduced in *Carm1* knockout embryos, providing a genetic link between estrogen action and CARM1.

We thank Drs. P. Leder, R. Weiss, D. Johnson, and A. Frankel for critical discussion; Gale Martin, Nahum Sonenberg, and Susan Dymecki for reagents; and Anne Harrington, Nancy Abbey, Jeff Everitt, and Deborah Hunter for additional help. M.T.B. is supported by National Institutes of Health Grant DK62248-01 and, in part, by institutional grants from the National Institute on Environmental Health Sciences (ES07784) and from the National Institutes of Health (CA16672).

- Aletta, J. M., Cimato, T. R. & Ettinger, M. J. (1998) *Trends Biochem. Sci.* **23**, 89–91.
- Gary, J. D. & Clarke, S. (1998) *Prog. Nucleic Acid Res. Mol. Biol.* **61**, 65–131.
- McBride, A. E. & Silver, P. A. (2001) *Cell* **106**, 5–8.
- Lin, W. J., Gary, J. D., Yang, M. C., Clarke, S. & Herschman, H. R. (1996) *J. Biol. Chem.* **271**, 15034–15044.
- Scott, H. S., Antonarakis, S. E., Lalioti, M. D., Rossier, C., Silver, P. A. & Henry, M. F. (1998) *Genomics* **48**, 330–340.
- Tang, J., Gary, J. D., Clarke, S. & Herschman, H. R. (1998) *J. Biol. Chem.* **273**, 16935–16945.
- Chen, D., Ma, H., Hong, H., Koh, S. S., Huang, S. M., Schurter, B. T., Aswad, D. W. & Stallcup, M. R. (1999) *Science* **284**, 2174–2177.
- Frankel, A., Yadav, N., Lee, J., Branscombe, T. L., Clarke, S. & Bedford, M. T. (2002) *J. Biol. Chem.* **277**, 3537–3543.
- Branscombe, T. L., Frankel, A., Lee, J. H., Cook, J. R., Yang, Z., Pestka, S. & Clarke, S. (2001) *J. Biol. Chem.* **276**, 32971–32976.
- Pollack, B. P., Kotenko, S. V., He, W., Izotova, L. S., Barnoski, B. L. & Pestka, S. (1999) *J. Biol. Chem.* **274**, 31531–31542.
- Chen, D., Huang, S. M. & Stallcup, M. R. (2000) *J. Biol. Chem.* **275**, 40810–40816.
- Koh, S. S., Chen, D., Lee, Y. H. & Stallcup, M. R. (2000) *J. Biol. Chem.* **276**, 1089–1098.
- Schurter, B. T., Koh, S. S., Chen, D., Bunick, G. J., Harp, J. M., Hanson, B. L., Henschen-Edman, A., Mackay, D. R., Stallcup, M. R. & Aswad, D. W. (2001) *Biochemistry* **40**, 5747–5756.
- Strahl, B. D., Briggs, S. D., Brame, C. J., Caldwell, J. A., Koh, S. S., Ma, H., Cook, R. G., Shabanowitz, J., Hunt, D. F., Stallcup, M. R. & Allis, C. D. (2001) *Curr. Biol.* **11**, 996–1000.
- Strahl, B. D. & Allis, C. D. (2000) *Nature* **403**, 41–45.
- Wang, H., Huang, Z. Q., Xia, L., Feng, Q., Erdjument-Bromage, H., Strahl, B. D., Briggs, S. D., Allis, C. D., Wong, J., Tempst, P. & Zhang, Y. (2001) *Science* **293**, 853–857.
- Daujatz, S., Bauer, U. M., Shah, V., Turner, B., Berger, S. & Kouzarides, T. (2002) *Curr. Biol.* **12**, 2090–2097.
- Chen, S. L., Löffler, K. A., Chen, D., Stallcup, M. R. & Muscat, G. E. (2002) *J. Biol. Chem.* **277**, 4324–4333.
- Koh, S. S., Li, H., Lee, Y. H., Wideltz, R. B., Chuong, C. M. & Stallcup, M. R. (2002) *J. Biol. Chem.* **277**, 26031–26035.
- Bauer, U. M., Daujat, S., Nielsen, S. J., Nightingale, K. & Kouzarides, T. (2002) *EMBO Rep.* **3**, 39–44.
- Ma, H., Baumann, C. T., Li, H., Strahl, B. D., Rice, R., Jelinek, M. A., Aswad, D. W., Allis, C. D., Hager, G. L. & Stallcup, M. R. (2001) *Curr. Biol.* **11**, 1981–1985.
- Lee, J. & Bedford, M. T. (2002) *EMBO Rep.* **3**, 268–273.
- Chevillard-Briet, M., Trouche, D. & Vandel, L. (2002) *EMBO J.* **21**, 5457–5466.
- Xu, W., Chen, H., Du, K., Asahara, H., Tini, M., Emerson, B. M., Montminy, M. & Evans, R. M. (2001) *Science* **294**, 2507–2511.
- Meyers, E. N., Lewandoski, M. & Martin, G. R. (1998) *Nat. Genet.* **18**, 136–141.
- McCarrick, J. W. D., Parnes, J. R., Seong, R. H., Solter, D. & Knowles, B. B. (1993) *Transgenic Res.* **2**, 183–190.
- Deng, C., Wynshaw-Boris, A., Zhou, F., Kuo, A. & Leder, P. (1996) *Cell* **84**, 911–921.
- Wood, S. A., Allen, N. D., Rossant, J., Auerbach, A. & Nagy, A. (1993) *Nature* **365**, 87–89.
- Weiss, R. S., Enoch, T. & Leder, P. (2000) *Genes Dev.* **14**, 1886–1898.
- Tzukerman, M. T., Esty, A., Santiso-Mere, D., Danielian, P., Parker, M. G., Stein, R. B., Pike, J. W. & McDonnell, D. P. (1994) *Mol. Endocrinol.* **8**, 21–30.
- Liu, Q. & Dreyfuss, G. (1995) *Mol. Cell. Biol.* **15**, 2800–2808.
- Weiss, V. H., McBride, A. E., Soriano, M. A., Filman, D. J., Silver, P. A. & Hogle, J. M. (2000) *Nat. Struct. Biol.* **7**, 1165–1171.
- Zhang, X., Zhou, L. & Cheng, X. (2000) *EMBO J.* **19**, 3509–3519.
- Kuivaniemi, P. C., Capulong, R. B., Harkins, R. N. & DeSombre, E. R. (1989) *Biochem. Biophys. Res. Commun.* **158**, 898–905.
- Sundstrom, S. A., Komm, B. S., Ponce-de-Leon, H., Yi, Z., Teuscher, C. & Lyttle, C. R. (1989) *J. Biol. Chem.* **264**, 16941–16947.
- Charpentier, A. H., Bednarek, A. K., Daniel, R. L., Hawkins, K. A., Laflin, K. J., Gaddis, S., MacLeod, M. C. & Aldaz, C. M. (2000) *Cancer Res.* **60**, 5977–5983.
- Bouras, T., Southey, M. C., Chang, A. C., Reddel, R. R., Willhite, D., Glynne, R., Henderson, M. A., Armes, J. E. & Venter, D. J. (2002) *Cancer Res.* **62**, 1289–1295.
- Lee, Y. H., Koh, S. S., Zhang, X., Cheng, X. & Stallcup, M. R. (2002) *Mol. Cell. Biol.* **22**, 3621–3632.
- Bedford, M. T., Reed, R. & Leder, P. (1998) *Proc. Natl. Acad. Sci. USA* **95**, 10602–10607.